nature structural & molecular biology

Structure of a human ASF1a–HIRA complex and insights into specificity of histone chaperone complex assembly

Yong Tang[1,4], Maxim V Poustovoitov[2,3,4], Kehao Zhao[1], Megan Garfinkel[2], Adrian Canutescu[2], Roland Dunbrack[2], Peter D Adams[2] & Ronen Marmorstein[1]

Human HIRA, ASF1a, ASF1b and CAF-1 are evolutionally conserved histone chaperones that form multiple functionally distinct chromatin-assembly complexes, with roles linked to diverse nuclear process, such as DNA replication and formation of heterochromatin in senescent cells. We report the crystal structure of an ASF1a–HIRA heterodimer and a biochemical dissection of ASF1a's mutually exclusive interactions with HIRA and the p60 subunit of CAF-1. The HIRA B domain forms an antiparallel β-hairpin that binds perpendicular to the strands of the β-sandwich of ASF1a, via β-sheet, salt bridge and van der Waals contacts. The N- and C-terminal regions of ASF1a and ASF1b determine the different affinities of these two proteins for HIRA, by contacting regions outside the HIRA B domain. CAF-1 p60 also uses B domain–like motifs for binding to ASF1a, thereby competing with HIRA. Together, these studies begin to define the molecular determinants of assembly of functionally diverse macromolecular histone chaperone complexes.

The basic repeating unit of eukaryotic chromatin is the core nucleosome. Each core nucleosome consists of a histone $(H3–H4)_2$ heterotetramer, two histone (H2A–H2B) heterodimers and about 147 base pairs of DNA. During chromatin assembly, histone chaperones donate histones to DNA[1]. In human cells, the deposition of the histone H3–H4 complex involves four histone chaperones: chromatin assembly factor-1 (CAF-1), histone regulatory homolog A (HIRA) and two antisilencing factor paralogs (ASF1a and ASF1b).

CAF-1, an evolutionarily conserved heterotrimeric chaperone comprised of p150, p60 and p48 subunits, mediates DNA synthesis–coupled chromatin assembly in S phase[1,2]. CAF-1 is also required for chromatin assembly coupled to DNA repair[3–8], for formation of specialized chromatin structures such as transcriptionally silent chromatin at telomeres, ribosomal DNA yeast mating loci and plant gene loci[3,9–12], and for proper pericentromeric chromatin structure in yeast[13].

The functions of the HIRA histone chaperone are substantially different from those of CAF-1. HIRA is the human ortholog of Hir proteins known to silence histone gene expression and create transcriptionally silent heterochromatin in yeast, flies, plants and humans[14–18]. In yeast, Hir1 and Hir2 also contribute to formation of pericentromeric chromatin structure[13]. However, the Hir-mediated silencing pathway is genetically separable from the CAF-1 pathway[16], and HIRA does not seem to participate in DNA replication–coupled or DNA repair–coupled chromatin assembly[19,20]. Instead, *in vitro* and during decondensation of the sperm pronucleus in flies, HIRA specifically deposits a histone variant, histone H3.3, independently of DNA replication and repair[19–21].

The ASF1 proteins share functions with both the CAF-1 and HIRA histone chaperones[16,22,23]. In human cells, there are two ASF1 paralogs, ASF1a and ASF1b, which are highly conserved in their N-terminal core domains but more diverged at their C-terminal tails (**Supplementary Fig. 1** online)[24]. ASF1a, but not ASF1b, physically interacts with HIRA, and this complex drives formation of specialized domains of facultative heterochromatin, called senescence-associated heterochromatin foci (SAHF), in senescent human cells[18,20]. Both ASF1 proteins also interact with CAF-1 p60 (refs. 22,25,26), and these interactions are thought to contribute to DNA replication–coupled and DNA repair–coupled chromatin assembly[26–29]. One role of ASF1 proteins in these complexes is to bind the histone H3–H4 complex[30,31]. Notably, the binding of HIRA and CAF-1 to ASF1 proteins seems to be mutually exclusive[20]. This exclusivity, as well as the specific binding of HIRA to ASF1a but not ASF1b, probably dictates the functional specialization of the CAF-1–containing and HIRA-containing chaperone complexes. Therefore, we set out to define the molecular basis of this specificity.

Previously, we have shown that HIRA specifically recognizes the N-terminal core domain of ASF1a via an evolutionarily conserved stretch of amino acid residues called the B domain[18,32]. Here, by mutagenic, biochemical and X-ray crystallographic approaches, we characterize this interface. We show that the HIRA B domain forms a β-hairpin that interacts extensively with the β-sandwich structure of the ASF1a N-terminal core domain through β-sheet, salt bridge and

[1]The Wistar Institute, Philadelphia, Pennsylvania 19104, USA. [2]The Fox Chase Cancer Center, Philadelphia, Pennsylvania 19111, USA. [3]Russian State Medical University, Moscow 117 869, Russia. [4]These authors contributed equally to this work. Correspondence should be addressed to R.M. (marmor@wistar.org) or P.D.A. (peter.adams@fccc.edu).

Received 5 May; accepted 28 August; published online 17 September 2006; doi:10.1038/nsmb1147

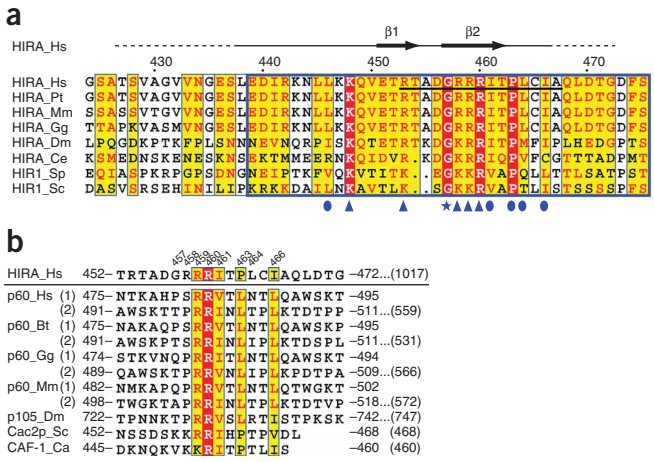

Figure 1 Sequence alignments of the B domains of HIRA and CAF-1 p60 homologs. (**a**) Extended B domains of HIRA homologs. Red highlight, strictly conserved (identical); yellow highlight, conserved (similar residues in red type); underline, minimal HIRA peptide required for ASF1a binding; blue box, core B domain, defined previously by sequence analysis and functional studies[18,32,33]. Residue numbering and secondary structure for human HIRA are indicated above alignment; black and dashed lines, ordered and disordered regions, respectively, of HIRA in the crystal structure. Blue symbols below mark HIRA residues that contact ASF1a: arrowhead, salt bridge; oval, hydrophobic; star, structural and/or non–salt bridge hydrogen bond. Bt, *Bos taurus*; Ca, *Candida albicans*; Ce, *Caenorhabditis elegans*; Dm, *D. melanogaster*; Gg, *Gallus gallus*; Hs, *Homo sapiens*; Mm, *Mus musculus*; Pt, *Pan troglodytes*; Sc, *Saccharomyces cerevisiae*; Sp, *Schizosaccharomyces pombe*. (**b**) B domain–like motifs of CAF-1 p60 homologs. For proteins with two motifs, both are aligned, designated (1) and (2). The human HIRA B domain is shown at top for comparison. HIRA residues that contact ASF1a are numbered above alignment. Starting and ending positions are marked on each sequence, with total number of residues in the full-length protein indicated in parentheses at right.

van der Waals interactions. We also define the molecular basis of HIRA's preference for ASF1a over ASF1b. Finally, we show that the CAF-1 p60 C terminus uses HIRA B domain–like motifs to recognize the same HIRA-binding surface on ASF1a, explaining why HIRA and CAF-1 p60 bind mutually exclusively to ASF1a to mediate distinct chromatin regulatory activities.

RESULTS

A minimum HIRA fragment that binds ASF1a

Wild-type human HIRA is a polypeptide of 1,017 residues. Previously, we have shown that residues 421–729 are sufficient for binding to the evolutionarily conserved N-terminal core domain of ASF1a, residues 1–155 (**Supplementary Fig. 1**), and for repression of histone gene expression and formation of SAHF in human cells[18,33]. This ASF1a-interacting domain of HIRA contains a stretch of about 37 residues that is evolutionarily conserved in HIRA and its orthologs and named the B domain (residues 439–475; **Fig. 1a**)[32]. The B domain is necessary for binding to ASF1a, repression of histone gene expression and formation of SAHF[18,33]. To date, the B domain has not been described outside of the HIRA family, although the p60 subunit of CAF-1 has some similarity to this domain (**Fig. 1b**).

To determine which region of the HIRA B domain makes crucial contacts with ASF1a, we made a series of scanning mutations, deleting 7–10 amino acids of the B domain at a time. The HA-tagged HIRA proteins were tested for binding to ASF1a *in vitro*. The two innermost deletions (of residues 449–458 and 459–468), encompassing the most highly conserved residues of the B domain (**Fig. 1a**), had the most debilitating effect on binding to ASF1a, whereas the two outermost deletions had a more modest effect (**Fig. 2a**).

Having identified the regions of the B domain that are necessary for binding to ASF1a, we next set out to define the minimum region of HIRA that is sufficient for binding. A series of HA-tagged deletion mutants derived from $HIRA_{421–729}$ were tested for binding to ASF1a. Constructs with C-terminal deletions as far as residue 509 all retained binding to ASF1a, although HA-$HIRA_{421–509}$ bound with reduced efficiency compared to HA-$HIRA_{421–729}$ (**Supplementary Fig. 2** online). An additional series of C-terminal deletion constructs were made, this time fused at their N termini to green fluorescent protein (GFP). Binding were retained with GFP-$HIRA_{421–479}$ but undetectable with GFP-$HIRA_{421–469}$ (**Fig. 2b**). We conclude that the minimum region of HIRA that retains binding to ASF1a lies within residues 421–479, underscoring the role of the B domain in ASF1a binding[32] (**Fig. 1a**).

Next, we examined whether a short peptide spanning the most conserved amino acid residues of the B domain is sufficient to interact with ASF1a, by testing its ability to compete with the binding of HA-$HIRA_{421–729}$ to ASF1a. Specifically, we tested residues 453–467 of wild-type HIRA, RTADGRRRITPLCIA, and a sequence-scrambled version, GRAARITPRDTLRCI, as a control. The wild-type peptide, but not the scrambled peptide, outcompeted the interaction between ASF1a and HA-$HIRA_{421–729}$ (**Fig. 2c**). Together, these results show that the B domain is both necessary and sufficient for interaction with ASF1a.

Structure of the ASF1a–HIRA complex

Having defined the minimal region of HIRA required for ASF1a interaction, we set out to determine the X-ray crystal structure of an ASF1a–HIRA complex. Toward this goal, we coexpressed the HIRA B domain (425–472) and the ASF1a N-terminal core domain (1–157) in *Escherichia coli* and purified the tightly associated heterodimeric complex to homogeneity. Crystals were obtained in the space group $P6_522$, containing two ASF1a–HIRA complexes per asymmetric unit. The structure of the complex was determined by molecular replacement using the crystal structure of the N-terminal core domain of yeast Asf1p[34] as a search model. This produced a clear solution for the two ASF1a molecules in the asymmetric unit and excellent density for

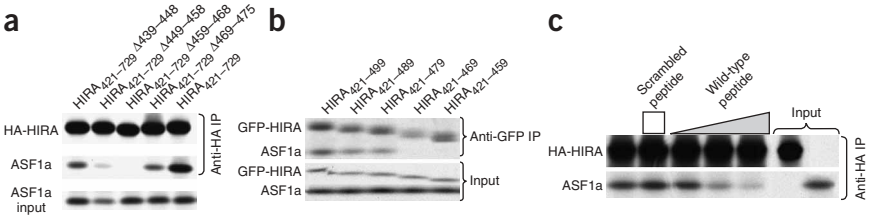

Figure 2 ASF1a binding to HIRA deletion constructs. (**a**) Binding of *in vitro*–translated ^{35}S-labeled HA-$HIRA_{421–729}$ and the indicated B domain deletion mutants to ^{35}S-labeled Myc-ASF1a. (**b**) Binding of *in vitro*–translated ^{35}S-labeled GFP-$HIRA_{421–729}$ and the indicated C-terminal deletion mutants to ^{35}S-labeled Myc-ASF1a. (**c**) Binding of *in vitro*–translated ^{35}S-labeled HA-$HIRA_{421–729}$ to ^{35}S-labeled Myc-ASF1a in the presence of 0, 1, 10 or 50 μg of the wild-type HIRA peptide, RTADGRRRITPLCIA, or 50 μg of the scrambled peptide, GRAARITPRDTLRCI. Heights of square and triangle indicate relative peptide concentrations.

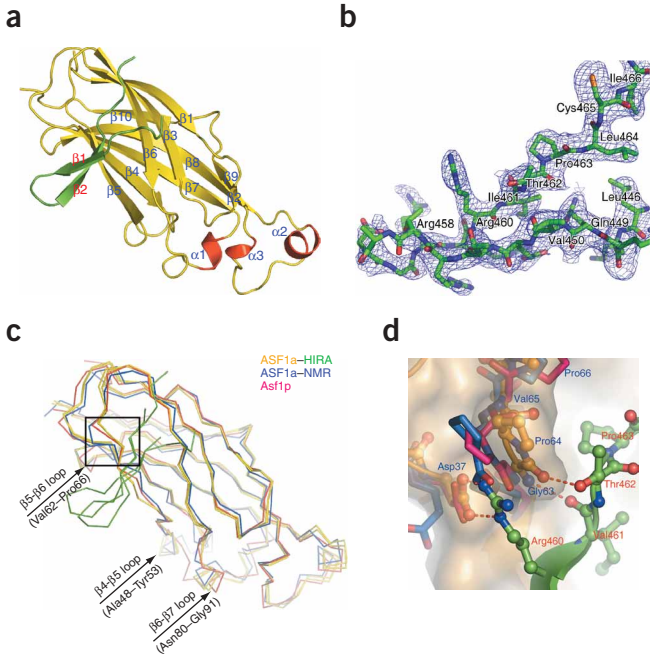

Figure 3 Overall structure of the ASF1a–HIRA complex and comparison with nascent yeast Asf1p and human ASF1a. (**a**) Ribbon representation of ASF1a–HIRA. ASF1a is in yellow, with the three helices in red and the bound HIRA fragment in green. (**b**) Section of the composite omit electron density map (contoured at 1.0 σ) of ASF1a–HIRA, showing a region of the HIRA fragment. (**c**) Cα superposition of the two ASF1a–HIRA complexes (ASF1a in yellow and HIRA in green) in the asymmetric unit with nascent structures of yeast Asf1p (red) and human ASF1a (blue). Black box defines the close-up region in **d**. (**d**) Close-up view of superposition in **c**, around the ASF1a 62-Val-Gly-Pro-64 triplet. Only one complex of the two ASF1aN–HIRA complexes in the asymmetric unit cell is shown, for clarity. Color-coding is as in **c** with CPK coloring and hydrogen bonds shown. **Figures 3**, **4a** and **7** were created with PyMOL (http://pymol.sourceforge.net).

the two ASF1a-bound HIRA fragments (**Fig. 3a**). One HIRA fragment could be built confidently into the electron density map from residue 446 to 466 and the other from residue 449 to 464 (**Fig. 3b**). We presume that the remainder of the HIRA fragment is disordered. The final model was refined to 2.7-Å resolution with excellent refinement statistics (see Methods).

The two ASF1a N-terminal core domains in the asymmetric unit (Cα r.m.s. deviation of 0.45 Å) adopt the same elongated immunoglobulin-like β-sandwich fold (**Fig. 3a**) previously described for the nascent structures of human ASF1a[31] and yeast Asf1p[34], with Cα r.m.s. deviations of 1.1 Å relative to both structures (**Fig. 3c**). However, variation between the free and HIRA-bound ASF1 polypeptides is evident at two less conserved loops (**Fig. 3c**) and, notably, also at the highly conserved β5-β6 loop at the HIRA interface (**Fig. 3d**). In particular, it appears that the β5-β6 turn of free ASF1a, especially around Gly63 and Pro64, is in a conformation that interferes with HIRA binding, but that it adjusts to accommodate the HIRA B domain upon complex formation.

Each of the two bound HIRA polypeptides in the asymmetric unit forms a β-hairpin containing two strands of 4 and 6 residues, respectively, with a 2-residue tight turn and loop extensions on the N- and C-terminal ends of the β-strands (**Fig. 3b**). In particular, residues Glu451–Thr454 and Gly457–Ile461 form a two-stranded antiparallel β-sheet that is stabilized by five intramolecular main chain and four side chain hydrogen bonds, including a bidentate salt bridge between residues Glu451 and Arg459 (**Fig. 4a**). Gly457 at the β-hairpin turn also adopts unique dihedral angles to facilitate two sets of hydrogen bonds between the backbone of Gly457 and residues Arg453 and Thr454 that stabilize the β-hairpin structure. The high degree of conservation of residues that mediate the intramolecular interactions within the β-hairpin of the HIRA B domain, and in particular the strict conservation of Gly457 (**Fig. 1a**), suggests that this structure may be preformed before ASF1a binding.

The B domain of HIRA binds along the edge and perpendicular to the strands of the β-sandwich of the ASF1a N-terminal core domain and makes extensive interactions with ASF1a, burying 652 Å^2 of HIRA surface (**Fig. 3a**). Both ASF1a–HIRA complexes in the asymmetric unit show similar contacts, despite the different HIRA conformations of residues around the β-hairpin turn (**Fig. 3c**). The HIRA-binding site on ASF1a is a shallow hydrophobic cleft that is primarily lined by residues Val60, Val62, Val65, Pro66, Phe72 and Phe74 from the β5-β6 region and Phe28 and Leu38 from the β3 and β4 strands, all involved in van der Waals interactions with residues Ile461, Pro463 and Leu464 of the HIRA B domain (**Fig. 4a**). There is also a cluster of salt bridges formed between the acidic residues Glu39, Asp58 and Asp37 of ASF1a and the basic residues Arg458, Arg459 and Arg460 of HIRA, respectively (**Fig. 4b**). Finally, residues Leu61–Gly63 of ASF1a (β5) form β-sheet interactions with residues Arg459–Ile461 (β2) of HIRA. The loops before and after the β-hairpin are both secured onto ASF1a by hydrogen bonds and hydrophobic interactions (**Fig. 4a**). Overall, it appears that HIRA residues Arg458–Ile466, which are included in the minimum ASF1a-binding peptide of HIRA (residues Arg453–Ala467) identified above, are most crucial in ASF1a interaction. Most of the ASF1a and HIRA residues involved in this interaction are either strictly or highly conserved (**Fig. 1a**

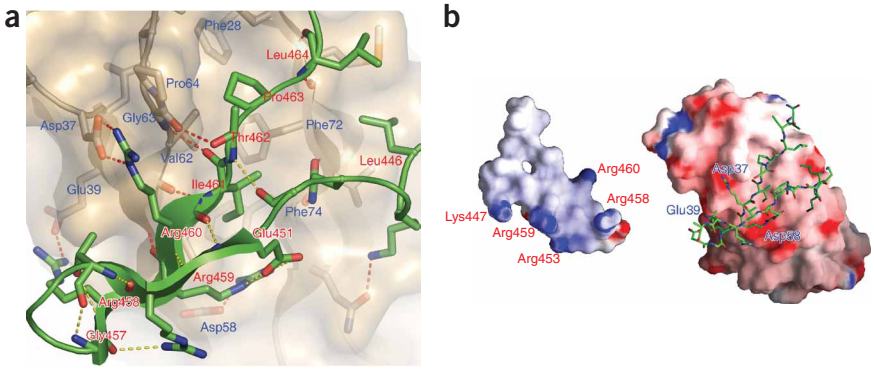

Figure 4 The ASF1a–HIRA interface. (**a**) Close-up view. ASF1a is shown as a gold ribbon and semitransparent surface representation and HIRA as a green ribbon. Residues from both molecules that mediate hydrogen bonds (including salt bridges) and hydrophobic interactions are shown as sticks with CPK coloring. Hydrogen bonds are shown as dashed lines (yellow, intramolecular; red, intermolecular). (**b**) Surface electrostatic representation of ASF1a and HIRA moieties in the complex. For clarity, the HIRA fragment in the complex is shown only as sticks with CPK coloring (right), with the HIRA surface shown in an open-book format (left). Residues involved in salt bridge interactions are indicated. This figure was made with GRASP[41].

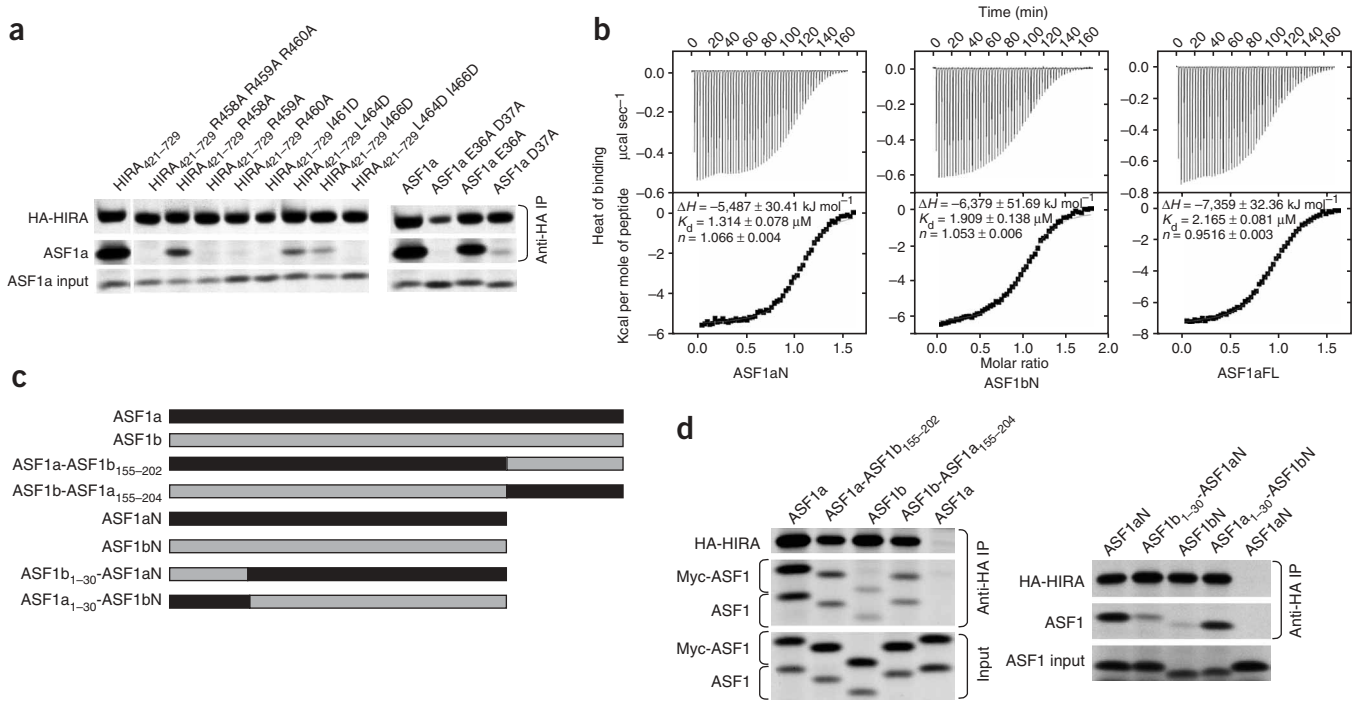

Figure 5 Functional characterization of the ASF1a-HIRA interaction. (**a**) Left, Binding of *in vitro*–translated ^{35}S-labeled HA-HIRA$_{421–729}$ and the indicated mutants to ^{35}S-labeled Myc-ASF1a. Right, binding of *in vitro*–translated ^{35}S-labeled HA-HIRA$_{421–729}$ to ^{35}S-labeled Myc-ASF1a or the indicated mutants. (**b**) Representative data from ITC assays of HIRA B domain peptide (residues 453–467) titrated into ASF1aN (residues 1–154), ASF1bN (residues 1–154) or ASF1aFL (full-length, residues 1–204). The area under each injection spike (top) is integrated and fitted using nonlinear least-squares regression analysis (bottom). Derived enthalpies (ΔH), dissociation constant (K_d) and stoichiometry (n) are indicated for each titration. This figure was prepared using Origin 5.0 (MicroCal). (**c**) Schematic of the protein chimeras used in **d**. (**d**) Binding of *in vitro*–translated ^{35}S-labeled HA-HIRA$_{421–729}$ to the indicated ^{35}S-labeled ASF1 proteins and their chimeras swapped at the C terminus (155–202; left) and N terminus (1–30; right).

and **Supplementary Fig. 1**), corroborating the importance of these contacts.

Biochemical characterization of the ASF1a–HIRA interface

Equipped with detailed structural insight into the ASF1a–HIRA interface, we then used targeted mutagenesis and *in vitro* binding assays to verify the functional significance of individual interactions between ASF1a and HIRA. We first examined the importance of the salt bridge interactions. Alanine substitution of either the second or third arginine in Arg458–Arg460 of HIRA, which interact with Asp58 and Asp37 of ASF1a, completely abolished binding (**Fig. 5a**). In addition, alanine substitution of the first arginine, Arg458, partially blocked binding. We then examined the corresponding contribution of the interacting residues in ASF1a. Previously, we have shown that double substitution of the acidic residues Glu36 and Asp37 with alanine residues abolishes binding to HIRA$_{421–729}$ (ref. 18). Consistent with the structural finding that only Asp37 is involved in salt bridge formation, the single substitution D37A abolished binding to HIRA$_{421–729}$, whereas E36A had little effect (**Fig. 5a**). Together, these results reveal that the charge interactions between highly conserved residues HIRA Arg460 and ASF1a Asp37, and HIRA Arg459 and ASF1a Asp58, are crucial for complex formation (**Fig. 1a** and **Supplementary Fig. 1**).

The role of the hydrophobic interactions between ASF1a and HIRA was also evaluated. Mutation of HIRA Ile461, one of two hydrophobic residues bound in the hydrophobic cleft of ASF1a, to aspartate abolished the interaction between HIRA$_{421–729}$ and ASF1a (**Fig. 5a**). In addition, mutation of either Leu464D or Ile466D in HIRA$_{421–729}$ partially blocked ASF1a binding, and mutation of both together completely abolished binding. Together, these findings agree with our structural finding that the hydrophobic cleft of ASF1a compliments Ile461 and Pro463 of HIRA, consistent with the strict evolutionary conservation of these two residues (**Fig. 1a**). An L464D I466D double mutant also disrupts ASF1a binding, suggesting that, although it is less conserved, this part of HIRA nonetheless has a role (**Fig. 5a**).

In an earlier study, we showed that mutation of the strictly conserved triplet Val62-Gly63-Pro64 to Ala-Ala-Ala, in the β5–β6 loop region of ASF1a, completely abolishes HIRA binding[34]. The structural comparison of the complex with free ASF1 proteins as described above suggested that the unique conformation and relative flexibility of this loop region is crucial for proper ASF1a-HIRA interactions. This mutation, largely by eliminating the unique conformations of Gly63 and *cis*-Pro64, not only disrupts direct hydrogen bonding with HIRA but also potentially causes steric occlusion of other contacts, such as the interaction between Asp37 of ASF1a and Arg460 of HIRA (**Figs. 3** and **4**). Taking all our results together, we conclude that a combination of β-sheet, electrostatic and hydrophobic interactions stabilizes the interaction between the ASF1a N-terminal core and the HIRA B domain.

Specificity of HIRA for ASF1a over ASF1b

In light of the earlier observations by us and other researchers that HIRA preferentially associates with ASF1a over ASF1b, *in vitro* and *in vivo*[18,20], we were surprised that each of the ASF1a residues involved in HIRA B domain binding are strictly conserved in ASF1b (**Supplementary Fig. 1**). This suggests that interactions between the

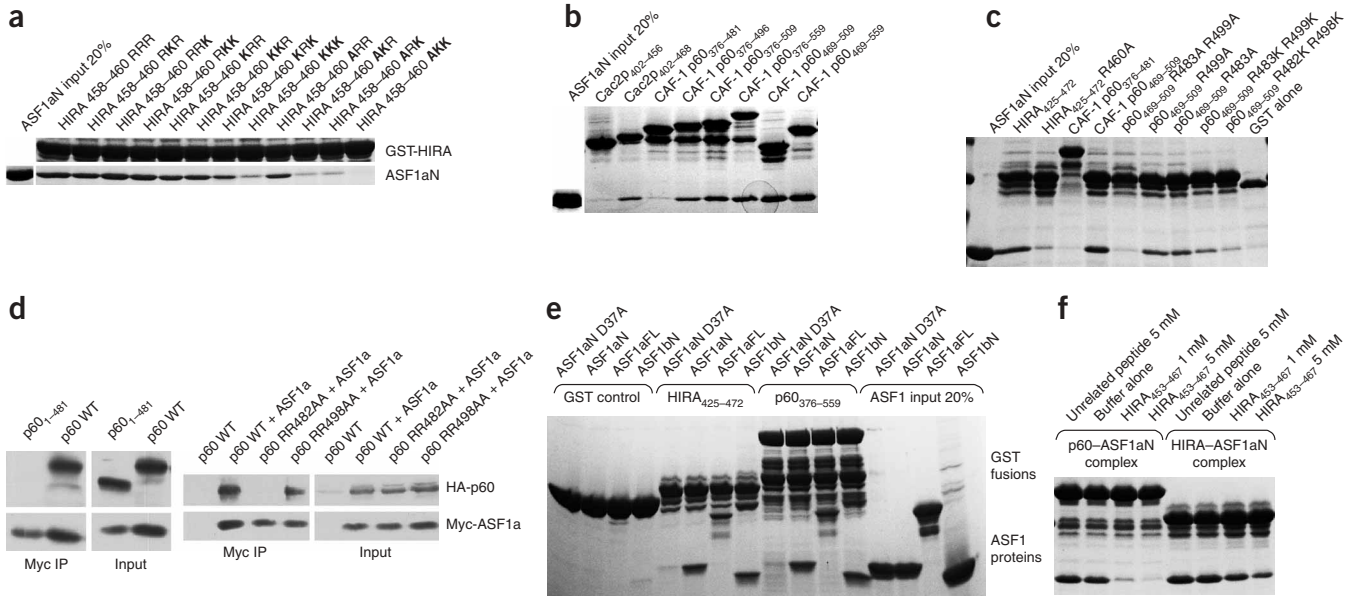

Figure 6 Functional characterization of ASF1a interaction with the HIRA B domain–like motifs of CAF-1 p60. (**a**) Binding of the GST-fused HIRA B domain and selected mutants to purified ASF1aN inputs. (**b**) Binding of affinity-purified GST-fused human CAF-1 p60 and yeast Cac2p to purified ASF1aN proteins. (**c**) Binding of affinity-purified GST-fused CAF-1 p60 and selected mutants to purified ASF1aN proteins. (**d**) Physical interactions between ectopically expressed CAF-1 p60 and ASF1a proteins in human U2OS cells, as tested by immunoprecipitation and western blot analysis. Left, interaction of HA-tagged wild-type CAF-1 p60 or truncation mutant $p60_{1–481}$ with Myc-tagged wild-type ASF1a. Right, interaction of HA-tagged CAF-1 p60 wild-type or mutant p60 R482A R483A (RR482AA) or p60 R498A R499A (RR498AA) with Myc-tagged wild-type ASF1a. (**e**) Binding of bacterially expressed, affinity-purified $HIRA_{425–472}$ and CAF-1 $p60_{376–559}$ GST fusion proteins to purified ASF1aN, ASF1bN, full-length ASF1a (ASF1aFL) or ASF1aN D37A mutant proteins. (**f**) Disruption of CAF-1 $p60_{469–559}$–ASF1aN and $HIRA_{425–472}$–ASF1aN complexes by a $HIRA_{453–467}$ peptide. In **b**, **c**, **e** and **f**, only the upper (intact) band of each individual GST fusion protein was used for evaluation of binding to ASF1a because of partial proteolysis of the fusion proteins during expression and purification.

ASF1a N-terminal core domain and the HIRA B domain are not responsible for HIRA's discrimination between ASF1a and ASF1b. To test this, we measured binding of the recombinant N-terminal core domains (residues 1–154) of ASF1a (ASF1aN) and ASF1b (ASF1bN) to the minimal HIRA B domain peptide (residues 453–467), using isothermal titration calorimetry (ITC). We also tested the full-length ASF1a protein, to evaluate the contribution of the C-terminal region of ASF1a to HIRA B domain binding. We were unable to prepare the full-length recombinant ASF1b protein in soluble form for ITC. The ITC studies show that the HIRA peptide binds with comparable affinity to each of the ASF1 proteins, with dissociation constants in the range of 1.3–2.1 μM (**Fig. 5b**). These results confirm that HIRA does not distinguish between ASF1a and ASF1b through the interaction between the HIRA B domain and the ASF1 N-terminal core domain. They further reveal that the C-terminal region of ASF1a does not influence binding of the HIRA B domain.

The ITC and structural studies together suggest that differential binding of ASF1a and ASF1b to HIRA might be mediated by regions outside the HIRA B domain or regions outside the B domain–interacting ASF1a core domain, or both. Previously, we have shown that simultaneous substitution into ASF1b of two regions of ASF1a that are relatively poorly conserved in ASF1b, residues 31–37 and the C-terminal 50 residues, potentiates binding of ASF1b to HIRA[18]. However, subsequent studies have revealed that substitution of residues 31–37 alone does not potentiate binding (data not shown). To further investigate the role of the nonconserved C-terminal tails of ASF1a and ASF1b (**Supplementary Fig. 1**) in HIRA binding, we tested binding of HA-tagged $HIRA_{421–729}$ to ASF1 chimeras in which the C-terminal tail regions of ASF1a and ASF1b were swapped (**Fig. 5c**). Swapping the C-terminal tails between ASF1a and ASF1b decreased binding of ASF1a but increased binding of ASF1b (**Fig. 5d**, left). From these results, we conclude that, in contrast to the ASF1b C-terminal tail, the ASF1a C terminus potentiates binding to HIRA.

Notably, in these HIRA binding studies, we observed that the ASF1a N-terminal core domain (lacking the C terminus; ASF1aN), the same region of ASF1a cocrystallized with HIRA, binds better to $HIRA_{421–729}$ than does ASF1bN (**Fig. 5c**,**d**). These results, coupled with our ITC studies showing that ASF1aN and ASF1bN bind indistinguishably to the HIRA B domain alone, suggest that another region of HIRA might bind ASF1aN. The N-terminal 30 residues of ASF1a and ASF1b are less conserved than the rest of the core domain (**Supplementary Fig. 1**) and lie in the vicinity of the HIRA B domain–binding surface (see below). To test whether this part of ASF1a mediates additional contacts with HIRA outside of the B domain and thus contributes to HIRA's specificity for ASF1a, we prepared chimeric proteins in which the N-terminal 30 residues were swapped between the ASF1a and ASF1b core domains and tested them for binding to $HIRA_{421–729}$. These experiments showed that ASF1bN carrying the N-terminal 30 residues of ASF1a binds $HIRA_{421–729}$ much better than does native ASF1bN (**Fig. 5d**, right). Conversely, ASF1aN carrying the N-terminal 30 residues of ASF1b binds $HIRA_{421–729}$ much worse than does native ASF1aN. From these results, we conclude that the N-terminal 30 residues of ASF1a and ASF1b contribute to the binding specificity for HIRA. Also, ASF1aN and $ASF1a_{1–30}$-ASF1bN have similarly high binding affinities for $HIRA_{421–729}$, whereas ASF1bN and $ASF1b_{1–30}$-ASF1aN have similarly low binding affinities (**Fig. 5d**, right), suggesting that residues 31–155 of ASF1a and ASF1b do not make direct contributions to their relative HIRA-binding specificities.

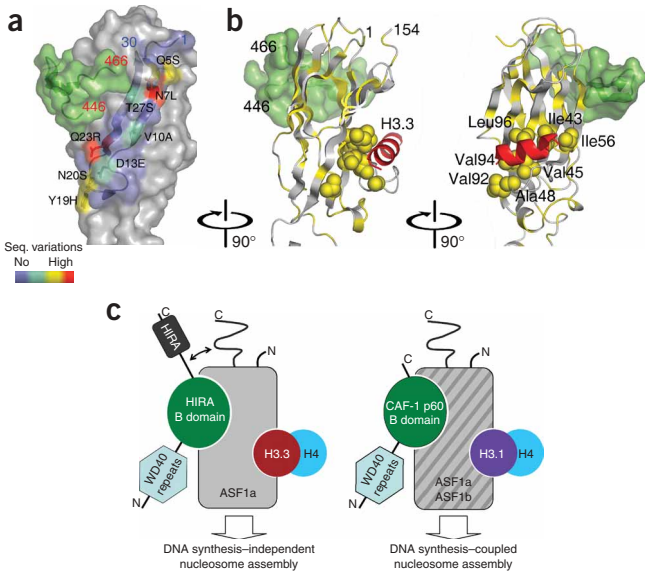

Figure 7 Model for binding of other HIRA regions and the histone H3.3 C-terminal helix to the HIRA B domain–ASF1a complex. (**a**) Surface representation of the ASF1a–HIRA complex, with residues 1–30 of ASF1a in blue. Color code highlights sequence variation between ASF1a and ASF1b as indicated in key. The HIRA fragment bound to ASF1a is also shown (green surface) for reference. (**b**) Hydrophobic residues (yellow) are mapped onto a ribbon representation of ASF1a, with the cluster of hydrophobic residues at the histone H3–binding site[31] shown as space-filling models. The HIRA fragment bound to ASF1a is shown as in **a**, and published NMR data[31] is used to model a histone H3 C-terminal helix (red) onto the ASF1a surface. Relative orientations of structures are indicated. (**c**) Schematic model for ASF1a and ASF1b association with HIRA, CAF-1 p60 and histone H3. See text for details.

In sum, our binding studies show that HIRA's discrimination between ASF1a and ASF1b depends on part(s) of the HIRA protein outside of the B domain and on both the N-terminal 30 residues and the C-terminal 50 residues of the ASF1 proteins.

B domain–like motifs in CAF-1 p60

Although ASF1a interacts with both HIRA and CAF-1 p60, it does not simultaneously copurify with both proteins[20]. Therefore, we hypothesized that CAF-1 p60 might bind ASF1a in an analogous fashion to HIRA, using a B domain–like motif. To test this, we searched CAF-1 p60 homologs for the consensus HIRA B domain motif, GRRRIXPLXI, that provides the crucial binding determinants for ASF1a. This search identified either one or two B domain–like motifs in the C-terminal tail of each of CAF-1 p60 homolog in the sequence database (**Fig. 1b**). Notably, a previous report has shown that the C-terminal region of the *Drosophila melanogaster* CAF-1 p60 homolog (p105), which also harbors this motif, mediates ASF1 binding[25].

Despite their overall similarity in the B domain and B domain–like regions, a very noticeable difference between HIRA and the CAF-1 p60 homologs is the lack of conservation among CAF-1 p60 homologs of the first and, to a lesser extent, the second of the three conserved arginine residues in HIRA (residues 458–460) (**Fig. 1a**,**b**). These residues make important salt bridge interactions with ASF1a in the complex (**Fig. 4a**). To assess the consequence of these differences, a series of mutations were generated in the 458-Arg-Arg-Arg-460 triplet of the HIRA B domain and the mutants tested for ASF1aN binding. Single or double Arg→Lys mutations within residues 458–460 did not markedly perturb ASF1a binding, whereas a triple Arg→Lys change resulted in a greater decrease (**Fig. 6a**). When Arg458 was mutated to alanine, to mimic the less polar residue found in the B domain–like motifs in CAF-1 p60, the HIRA B domain still maintained a relatively high level of ASF1aN binding (**Fig. 6a**). However, when the R458A mutation was combined with either the R459K or R460K mutation, ASF1a binding was substantially impaired, albeit not abolished (**Fig. 6a**). A combination of the R458A mutation with the R459K R460K double mutation completely abolishes ASF1aN binding (**Fig. 6a**), indicating that in the absence of a basic residue at position 458, maintaining at least one arginine (instead of lysine) at either position 459 or 460 is crucial for ASF1aN binding. These results suggest that the B domain–like motifs of CAF-1 p60 and its homologs could mediate binding of the corresponding proteins to ASF1aN.

To directly determine whether the two B domain–like motifs in human CAF-1 p60 (residues 480–490 and 496–506) mediate ASF1a binding, various CAF-1 p60 C-terminal fragments were tested for binding to the ASF1a N-terminal core domain. CAF-1 p60 fragments containing both B domain–like motifs (residues 376–509, 376–559, 469–509 and 469–559) interact with ASF1a, whereas a polypeptide with both motifs deleted (376–481) binds very weakly (**Fig. 6b**). A fragment harboring only the first B domain–like motif (376–496) binds with slightly reduced affinity relative to the fragments harboring both motifs. ASF1a pull-down experiments with the yeast CAF-1 p60 homolog, Cac2p, showed that this protein also interacts with ASF1a, via a conserved B domain–like motif (residues 457–468; **Fig. 6b**). Together, these studies show that human and yeast CAF-1 p60 bind the conserved ASF1a core domain through their evolutionarily conserved C-terminal B domain–like motifs.

To verify that ASF1a interacts with both HIRA and CAF-1 p60 through the B domain motifs and to establish the relative importance of the first and second B domain–like motifs in CAF-1 p60, we carried out ASF1a pull-down studies with the shortest CAF-1 p60 fragment (469–509) that contains both motifs. We used versions of this fragment harboring mutations of the arginine residues in both motifs, Arg483 and Arg499, that are equivalent to the crucial Arg460 in HIRA. The R483A R499A double mutation in CAF-1 p60 abolishes the ASF1a interaction, and a comparable double mutation to lysine markedly compromises it (**Fig. 6c**). Pull-down experiments with single R483A and R499A mutations of CAF-1 p60 revealed similar residual ASF1a-binding capacities (**Fig. 6c**), indicating that either B domain–like motif of CAF-1 p60 can bind ASF1a *in vitro* in the context of this minimal CAF-1 p60 fragment.

To test whether other regions of CAF-1 p60 participate in ASF1a binding and to investigate whether both B domain–like motifs of CAF-1 p60 contribute to ASF1a binding in the intact full-length CAF-1 p60 protein and *in vivo*, we carried out coimmunoprecipitation assays using epitope-tagged CAF-1 p60 proteins ectopically expressed in U2OS cells. Specifically, we used native full-length CAF-1 p60, full-length proteins containing RR→AA mutations in either the first or second B domain–like motif (R482A R483A or R498A R499A, respectively), and a fragment harboring the N-terminal WD40 repeats but not the two C-terminal B domain–like motifs (residues 1–481). Whereas wild-type CAF-1 p60 has strong binding activity, CAF-1 $p60_{1–481}$ is completely inactive in ASF1a binding (**Fig. 6d**, left), indicating that the N-terminal WD40 repeats are not sufficient for ASF1a binding and that the C-terminal region, harboring the two B domain–like motifs, is crucial. Intact CAF-1 p60 harboring the RR→AA mutation in the second B domain–like motif binds ASF1a

with wild-type efficiency, whereas mutation of the first B domain–like motif completely abolished binding (**Fig. 6d**, right). Taking all our results together, we conclude that, in the context of the full-length CAF-1 p60 protein *in vivo*, the first B domain–like motif of CAF-1 is primarily responsible for ASF1a binding.

We next compared CAF-1 p60 binding to ASF1a and ASF1b, using a fragment of CAF-1 p60 missing only the N-terminal WD40 repeats (residues 376–559), as these repeats are neither necessary nor sufficient for ASF1a binding (**Fig. 6b,d**). CAF-1 $p60_{376–559}$ binds equally well to ASF1aN, ASF1bN and full-length ASF1a (**Fig. 6e**), consistent with earlier findings that CAF-1 p60 associates with both ASF1a and ASF1b *in vivo*[20].

Additional binding experiments using the ASF1aN D37A mutant, a mutant that does not bind HIRA (**Fig. 5a**), were also carried out. These experiments revealed that the ASF1aN D37A mutant does not bind CAF-1 $p60_{376–559}$ or the HIRA B domain, indicating that CAF-1 p60 makes interactions with the ASF1a and ASF1b core domains that are analogous to interactions of the HIRA B domain with ASF1a.

These data suggest that the HIRA B domain and the B domain–like motifs of CAF-1 p60 bind the ASF1a core domain in similar and, therefore, mutually exclusive fashions. To directly test this, we purified ASF1aN–$HIRA_{425–472}$ and ASF1aN–CAF-1 $p60_{469–559}$ complexes and mixed them with increasing concentrations of HIRA peptide (453–467; 0, 1 and 5 mM). The HIRA peptide displaced the majority of the CAF-1 $p60_{469–559}$ fragment and moderately displaces the HIRA B domain (425–472) from ASF1a (**Fig. 6f**). An unrelated peptide did not displace either HIRA or CAF-1 p60 at the highest concentration (**Fig. 6f**). This confirms that HIRA and CAF-1 p60 bind mutually exclusively to the N-terminal core of ASF1a.

DISCUSSION

Here we have presented structural and functional data to define the essential interaction interface between two histone chaperones, HIRA and ASF1a, that function as a complex *in vivo*. In the process, we discovered that the B domain, previously defined only in human HIRA and its orthologs, is conserved as an ASF1-binding motif in CAF-1 p60 proteins from yeast to human. Moreover, we found that HIRA's specific binding to ASF1a, but not ASF1b, is dictated by flanking sequences outside of the core interaction domains of both proteins. The structure of the ASF1a–HIRA complex reveals that the N-terminal 30 residues of ASF1 drape across the long axis of the elongated ASF1a core domain and are in position to interact with regions on the N- and C-terminal sides of the HIRA B domain that would contact this region of ASF1a (**Fig. 7a**). Without structural information on the C-terminal tail region of ASF1a, which we show is also involved in HIRA binding, we are unable to assign its position relative to the core domain upon HIRA binding, but we propose that it may be adjacent to the ASF1aN–HIRA B domain interface (**Fig. 7c**). Thus, the B domain of HIRA defines a conserved ASF1-binding motif whose specificity is modified by other sequences within both the ASF1 protein and HIRA itself.

We identified B domain–like motifs in CAF-1 p60 that mediate an interaction with ASF1a that is mutually exclusive with the HIRA interaction, suggesting that both HIRA and CAF-1 compete for ASF1a association *in vivo* to promote their distinct ASF1a-mediated chromatin regulatory activities. We further verified that although both B domain–like motifs of p60 contain the sequence determinants for ASF1a association, only the first motif is involved in ASF1a association in the context of the full-length CAF-1 p60 protein *in vivo*. This suggests a 1:1 stoichiometry of the ASF1a–CAF-1 p60 complex, similar to that of the ASF1a–HIRA complex. However, our sequence comparisons, binding assays and peptide-displacement studies also indicate that the CAF-1 p60 B domain has a lower binding affinity for ASF1aN than does the HIRA B domain (**Fig. 6a–f**), probably owing to differences at residues equivalent to HIRA Arg458, Ile461 and Leu464, which are involved in important charge or hydrophobic interactions with ASF1a.

The physiological relevance of our finding that ASF1a binds both HIRA and CAF-1 p60 through the same domain is reinforced by a recent cellular study[35]. This study reports that an ASF1a E36A D37A mutant, when stably expressed in a conditional ASF1a-knockout chicken DT40 cell line, does not interact with CAF-1 p60. The authors also show *in vitro* that ASF1a E36A D37A does not bind wild-type HIRA. We have previously shown *in vitro* and *in vivo* that neither ASF1a E36A D37A nor a HIRA mutant lacking the B domain interacts with its wild-type cognate binding partner[18].

A recent NMR chemical shift analysis of ASF1a, in the absence and presence of the histone H3 C-terminal helix, identified the histone H3–binding surface of ASF1a as a hydrophobic surface on the β4 loop and β7 strand of ASF1a, a result confirmed by mutagenesis studies[31]. On the basis of these results, it seems that the histone H3–H4 complex and HIRA bind on opposite faces of ASF1a (**Fig. 7b**). This is consistent with mutational data showing that the D37R E39R double mutation that disrupts the ASF1a-HIRA interaction does not affect the interaction between ASF1a and histone H3 (ref. 31). A schematic model of the ASF1a interaction with HIRA, CAF-1 p60 and histone H3 that incorporates our findings is presented in **Figure 7c**. Key features of this model are that (i) HIRA and CAF-1 p60 use analogous B domains to compete for the same binding surface on ASF1a; (ii) HIRA regions outside of the B domain participate in ASF1a binding via interaction with the N- and C-terminal fragments of ASF1a, potentiating HIRA's specificity for ASF1a over ASF1b, whereas CAF-1 p60 binds comparably to ASF1a and ASF1b; and (iii) the B domain–binding surface of ASF1 proteins lies away from their histone H3–H4–binding surface but nonetheless may communicate through other regions of ASF1.

Future structural and biochemical studies comparable to those reported here would uncover additional principles that guide the assembly and activity of multisubunit histone chaperone complexes. In sum, we have begun to define such principles for two complexes that are functionally distinct. These principles, together with the use of additional targeting and regulatory subunits, no doubt contribute to the cell's ability to target functionally specific histone chaperone complexes to chromatin at the correct time and place.

METHODS

Molecular cloning and protein expression. Genes encoding full-length human ASF1 proteins and N-terminal core domains of human ASF1a (residues 1–157) and human ASF1b (residues 1–154) were cloned into a modified pET Duet vector (Novagen) with a Thrombin/TEV-cleavable His_6 tag. The HIRA B domain (residues 425–472) and various CAF-1 p60 and Cac2p constructs were cloned into a modified pCDF Duet vector (Novagen) with a thrombin/TEV-cleavable N-terminal glutathione *S*-transferase (GST) fusion. The complementary DNA fragments coding for the HIRA and ASF1 proteins to be translated *in vitro* were amplified by PCR and subcloned into pcDNA3 (Invitrogen) or pSG5 (Stratagene). Selected point mutations described in the text were introduced by site-directed mutagenesis using the QuikChange mutagenesis kit according to the manufacturer's protocol (Invitrogen) or by two-step mutagenic PCR, and constructs were sequenced to confirm mutations.

Recombinant proteins were expressed in BL21-Gold (DE3) cells at 37 °C for 3 h or at 18 °C overnight. ASF1a–HIRA and ASF1a–CAF-1 p60 complexes were produced by coexpression. After standard GST- or His_6-tagged protein affinity purifications, proteins were cleaved by thrombin or TEV protease

Table 1 Data collection and refinement statistics

	Human ASF1a–HIRA complex
Data Collection	
Wavelength (Å)	0.980
Space group	$P6_522$
Cell dimensions	
a, b, c (Å)	116.2, 116.2, 167.6
α, β, γ (°)	90.0, 90.0,120.0
Resolution (Å)	25–2.7 (2.8–2.7)
R_{merge}	0.037 (0.315)
$I / \sigma I$	42.6 (5.3)
Completeness (%)	100 (100)
Redundancy	8.4 (8.6)
Refinement	
Resolution (Å)	2.7
No. reflections	19,106
R_{work} / R_{free}	22.9 / 26.9
No. atoms	
Proteins (ASF1a / HIRA)	2,784 (2,482 / 302)
Water	130
B-factors	
Proteins (ASF1a / HIRA)	53.1 (53.1 / 53.0)
Water	49.4
R.m.s deviations	
Bond lengths (Å)	0.0067
Bond angles (°)	1.421

Values in parentheses are for the highest-resolution shell.

when necessary and then further purified by ion-exchange and gel-filtration chromatography. The $HIRA_{453–467}$ peptide was synthesized using Fmoc on solid phase, purified using reversed-phase HPLC and confirmed by mass spectrometry (Wistar Institute, Proteomics Core Facility).

Isothermal titration calorimetry. ASF1 proteins (0.025 mM) and HIRA peptide (0.2 mM) were dialyzed against PBS-βME (1× PBS, 5 mM β-mercaptoethanol) before ITC analysis. HIRA peptide was titrated into ASF1a proteins at 15 °C with 56 injections (5 μl each), with other methodological details essentially as described[36].

***In vitro* binding assays.** Selected GST fusion proteins expressed in 5-ml *E. coli* cultures were purified by and retained on 100 μl glutathione sepharose beads and washed five times with PBS-βME. Samples were quantitated by SDS-PAGE analysis before the addition of excess stoichiometric amounts of ASF1aN or the D37A mutant. Binding reactions were incubated at 4 °C for 2 h with gentle rotation before washing three times with PBS-βME, then washing two more times with PBS-βME plus 160 mM NaCl and 0.05% (v/v) Tween 20. Samples from the last wash were resolved by SDS-PAGE and visualized by Coomassie blue staining.

^{35}S-labeled *in vitro*–translated proteins were derived from pcDNA3- or pSG5-based plasmids using the Promega Transcription and Translation kit, according to the manufacturer's instructions. Binding assays and peptide competition experiments were performed as described[37]. Antibodies to HA (12CA5) and Myc (9E10) were from Santa Cruz.

For B domain binding competition experiments, ASF1aN–$HIRA_{425–472}$ and ASF1aN–CAF-1 $p60_{469–559}$ complexes were prepared as described above. Four aliquots of about 100 μg of each complex were retained on 100 μl of glutathione beads in PBS-βME, and an increasing amount of the HIRA B domain peptide was added to each aliquot to a final volume of 0.5 ml and incubated at 4 °C for 3 h. Beads were washed three times with PBS-βME and analyzed by SDS-PAGE to evaluate the displacement of ASF1a from the beads that was caused by the competitive binding of $HIRA_{453–467}$ peptide to ASF1aN previously bound to either CAF-1 $p60_{469–559}$ or $HIRA_{425–472}$.

Transfections and immunoprecipitations. Human U2OS cells were cultured and transfected with pcDNA3 (Invitrogen)-based plasmids encoding epitope-tagged CAF-1 p60 and ASF1a proteins as described[18]. Immunoprecipitations and western blots with antibodies to HA (Y11, Santa Cruz) and Myc (9E10, Santa Cruz) were also performed as described[18].

Crystallization, data collection, structure determination and refinement. Crystals of the human ASF1aN–$HIRA_{425–472}$ complex were grown by hanging drop vapor diffusion at room temperature and were obtained by mixing 2 μl of a 0.5-mM protein complex solution (in 20 mM HEPES (pH 7.0), 150 mM NaCl and 5 mM βME) with 2 μl of reservoir solution containing 1.44 M NaH_2PO4 and 0.16 M K_2HPO4 at pH 5.6 and equilibrating over 1.0 ml of reservoir solution. Crystals were fully grown within 2 weeks to a typical size of 0.3 mm × 0.3 mm × 0.2 mm and were cryo-protected for data collection by stepwise transfer into reservoir solutions supplemented with 15%–25% (v/v) glycerol. Diffraction data from the crystals was obtained at beamline X6A at the National Synchrotron Light Source at Brookhaven National Laboratory. All data was processed with the HKL 2000 suite (HKL Research). The structure was solved by molecular replacement with PHASER[38], using protein residues 1–154 from the yeast Asf1 protein structure[34] as a search model. The structure was refined by simulated annealing, torsion-angle dynamics and *B*-factor adjustments in CNS[39], with iterative manual adjustments of the model and placement of solvent molecules using O[40]. The final model was checked for errors with composite simulated annealing omit maps, and a final round of refinement resulted in a model with excellent refinement statistics and geometry (**Table 1**). For the two HIRA fragments in the asymmetric unit, residues 425–445 and 467–472, and 425–448 and 465–472 are missing, respectively. The two ASF1a molecules both have residues 155-157 missing.

Accession codes. Protein Data Bank: Coordinates have been deposited with accession code 2I32.

Note: Supplementary information is available on the Nature Structural & Molecular Biology website.

ACKNOWLEDGMENTS

We thank M. Allaire for assistance with data collection. This work was supported by US National Institutes of Health grants to R.M. and P.D.A., a Leukemia and Lymphoma Society Scholar Award to P.D.A. and a grant from the Commonwealth Universal Research Enhancement Program, Pennsylvania Department of Health, awarded to the Wistar Institute. Part of this research was conducted on beamline X6A at the National Synchrotron Light Source at Brookhaven National Laboratory, which is supported by the US Department of Energy under contract no. DE-AC02-98CH10886. Beamline X6A is funded by the US National Institutes of Health, National Institute of General Medical Sciences, under agreement Y1 GM-0080-03.

AUTHOR CONTRIBUTIONS

Y.T. and M.V.P. designed and carried out the reported experiments and prepared manuscript figures and text; K.Z., M.G., A.C. and R.D. carried out preliminary studies that led to the reported experiments; P.D.A and R.M. designed and supervised experiments and prepared manuscript text. All authors read and approved the submitted manuscript.

COMPETING INTERESTS STATEMENT

The authors declare that they have no competing financial interests.

Published online at http://www.nature.com/nsmb/
Reprints and permissions information is available online at http://npg.nature.com/reprintsandpermissions/

1. Loyola, A. & Almouzni, G. Histone chaperones, a supporting role in the limelight. *Biochim. Biophys. Acta* **1677**, 3–11 (2004).
2. Smith, S. & Stillman, B. Purification and characterization of CAF-I, a human cell factor required for chromatin assembly during DNA replication *in vitro*. *Cell* **58**, 15–25 (1989).
3. Kaufman, P.D., Kobayashi, R. & Stillman, B. Ultraviolet radiation sensitivity and reduction of telomeric silencing in *Saccharomyces cerevisiae* cells lacking chromatin assembly factor-I. *Genes Dev.* **11**, 345–357 (1997).
4. Linger, J. & Tyler, J.K. The yeast histone chaperone chromatin assembly factor 1 protects against double-strand DNA-damaging agents. *Genetics* **171**, 1513–1522 (2005).
5. Myung, K., Pennaneach, V., Kats, E.S. & Kolodner, R.D. *Saccharomyces cerevisiae* chromatin-assembly factors that act during DNA replication function in the

maintenance of genome stability. *Proc. Natl Acad. Sci. USA* **100**, 6640–6645 (2003).
6. Gaillard, P.H. *et al.* Chromatin assembly coupled to DNA repair: a new role for chromatin assembly factor I. *Cell* **86**, 887–896 (1996).
7. Moggs, J.G. *et al.* A CAF-1-PCNA-mediated chromatin assembly pathway triggered by sensing DNA damage. *Mol. Cell. Biol.* **20**, 1206–1218 (2000).
8. Green, C.M. & Almouzni, G. Local action of the chromatin assembly factor CAF-1 at sites of nucleotide excision repair *in vivo*. *EMBO J.* **22**, 5163–5174 (2003).
9. Enomoto, S., McCune-Zierath, P.D., Gerami-Nejad, M., Sanders, M.A. & Berman, J. RLF2, a subunit of yeast chromatin assembly factor-I, is required for telomeric chromatin function in vivo. *Genes Dev.* **11**, 358–370 (1997).
10. Enomoto, S. & Berman, J. Chromatin assembly factor I contributes to the maintenance, but not the re-establishment, of silencing at the yeast silent mating loci. *Genes Dev.* **12**, 219–232 (1998).
11. Monson, E.K., de Bruin, D. & Zakian, V.A. The yeast Cac1 protein is required for the stable inheritance of transcriptionally repressed chromatin at telomeres. *Proc. Natl Acad. Sci. USA* **94**, 13081–13086 (1997).
12. Kaya, H. *et al.* FASCIATA genes for chromatin assembly factor-1 in *Arabidopsis* maintain the cellular organization of apical meristems. *Cell* **104**, 131–142 (2001).
13. Sharp, J.A., Franco, A.A., Osley, M.A. & Kaufman, P.D. Chromatin assembly factor I and Hir proteins contribute to building functional kinetochores in *S. cerevisiae*. *Genes Dev.* **16**, 85–100 (2002).
14. Kaufman, P.D., Cohen, J.L. & Osley, M.A. Hir proteins are required for position-dependent gene silencing in *Saccharomyces cerevisiae* in the absence of chromatin assembly factor I. *Mol. Cell. Biol.* **18**, 4793–4806 (1998).
15. Phelps-Durr, T.L., Thomas, J., Vahab, P. & Timmermans, M.C. Maize rough sheath2 and its *Arabidopsis* orthologue ASYMMETRIC LEAVES1 interact with HIRA, a predicted histone chaperone, to maintain *knox* gene silencing and determinacy during organogenesis. *Plant Cell* **17**, 2886–2898 (2005).
16. Sharp, J.A., Fouts, E.T., Krawitz, D.C. & Kaufman, P.D. Yeast histone deposition protein Asf1p requires Hir proteins and PCNA for heterochromatic silencing. *Curr. Biol.* **11**, 463–473 (2001).
17. Sherwood, P.W., Tsang, S.V. & Osley, M.A. Characterization of *HIR1* and *HIR2*, two genes required for regulation of histone gene transcription in *Saccharomyces cerevisiae*. *Mol. Cell. Biol.* **13**, 28–38 (1993).
18. Zhang, R. *et al.* Formation of MacroH2A-containing senescence-associated heterochromatin foci and senescence driven by ASF1a and HIRA. *Dev. Cell* **8**, 19–30 (2005).
19. Ray-Gallet, D. *et al.* HIRA is critical for a nucleosome assembly pathway independent of DNA synthesis. *Mol. Cell* **9**, 1091–1100 (2002).
20. Tagami, H., Ray-Gallet, D., Almouzni, G. & Nakatani, Y. Histone H3.1 and H3.3 complexes mediate nucleosome assembly pathways dependent or independent of DNA synthesis. *Cell* **116**, 51–61 (2004).
21. Loppin, B. *et al.* The histone H3.3 chaperone HIRA is essential for chromatin assembly in the male pronucleus. *Nature* **437**, 1386–1390 (2005).
22. Sutton, A., Bucaria, J., Osley, M.A. & Sternglanz, R. Yeast ASF1 protein is required for cell cycle regulation of histone gene transcription. *Genetics* **158**, 587–596 (2001).
23. Tyler, J.K. *et al.* The RCAF complex mediates chromatin assembly during DNA replication and repair. *Nature* **402**, 555–560 (1999).
24. Sillje, H.H. & Nigg, E.A. Identification of human Asf1 chromatin assembly factors as substrates of Tousled-like kinases. *Curr. Biol.* **11**, 1068–1073 (2001).
25. Tyler, J.K. *et al.* Interaction between the *Drosophila* CAF-1 and ASF1 chromatin assembly factors. *Mol. Cell. Biol.* **21**, 6574–6584 (2001).
26. Mello, J.A. *et al.* Human Asf1 and CAF-1 interact and synergize in a repair-coupled nucleosome assembly pathway. *EMBO Rep.* **3**, 329–334 (2002).
27. Krawitz, D.C., Kama, T. & Kaufman, P.D. Chromatin assembly factor I mutants defective for PCNA binding require Asf1/Hir proteins for silencing. *Mol. Cell. Biol.* **22**, 614–625 (2002).
28. Schulz, L.L. & Tyler, J.K. The histone chaperone ASF1 localizes to active DNA replication forks to mediate efficient DNA replication. *FASEB J.* **20**, 488–490 (2006).
29. Franco, A.A., Lam, W.M., Burgers, P.M. & Kaufman, P.D. Histone deposition protein Asf1 maintains DNA replisome integrity and interacts with replication factor C. *Genes Dev.* **19**, 1365–1375 (2005).
30. Munakata, T., Adachi, N., Yokoyama, N., Kuzuhara, T. & Horikoshi, M. A human homologue of yeast anti-silencing factor has histone chaperone activity. *Genes Cells* **5**, 221–233 (2000).
31. Mousson, F. *et al.* Structural basis for the interaction of Asf1 with histone H3 and its functional implications. *Proc. Natl Acad. Sci. USA* **102**, 5975–5980 (2005).
32. Kirov, N., Shtilbans, A. & Rushlow, C. Isolation and characterization of a new gene encoding a member of the HIRA family of proteins from *Drosophila melanogaster*. *Gene* **212**, 323–332 (1998).
33. Nelson, D.M. *et al.* Coupling of DNA synthesis and histone synthesis in S phase independent of cyclin/cdk2 activity. *Mol. Cell. Biol.* **22**, 7459–7472 (2002).
34. Daganzo, S.M. *et al.* Structure and function of the conserved core of histone deposition protein Asf1. *Curr. Biol.* **13**, 2148–2158 (2003).
35. Sanematsu, F. *et al.* Asf1 is required for viability and chromatin assembly during DNA replication in vertebrate cells. *J. Biol. Chem.* **281**, 13817–13827 (2006).
36. Zhao, K., Harshaw, R., Chai, X. & Marmorstein, R. Structural basis for nicotinamide cleavage and ADP-ribose transfer by NAD(+)-dependent Sir2 histone/protein deacetylases. *Proc. Natl Acad. Sci. USA* **101**, 8563–8568 (2004).
37. Adams, P.D. *et al.* Identification of a cyclin-cdk2 recognition motif present in substrates and p21-like cyclin-dependent kinase inhibitors. *Mol. Cell. Biol.* **16**, 6623–6633 (1996).
38. McCoy, A.J., Grosse-Kunstleve, R.W., Storoni, L.C. & Read, R.J. Likelihood-enhanced fast translation functions. *Acta Crystallogr. D Biol. Crystallogr.* **61**, 458–464 (2005).
39. Brunger, A.T. *et al.* Crystallography & NMR system: a new software suite for macromolecular structure determination. *Acta Crystallogr. D Biol. Crystallogr.* **54**, 905–921 (1998).
40. Jones, T.A., Zou, J.Y., Cowan, S.W. & Kjeldgaard, M. Improved methods for building protein models in electron density maps and the location of errors in these models. *Acta Crystallogr. A* **47**, 110–119 (1991).
41. Nicholls, A., Sharp, K. & Honig, B. GRASP-graphical representation and analysis of surface properties. *Proteins Struct. Funct. Genet.* **11**, 281ff (2003).